SPECTROSCOPY OF ^{125}Te WITH (n,γ), (d,p) AND (^{3}He,α) REACTIONS

JAROSLAV HONZÁTKO[a], IVO TOMANDL[a], VALERIE BONDARENKO[b,1], JÜRGEN OTT[b],
TILL von EGIDY[b], WERNER SCHAUER[b], CHRISTIAN DOLL[b], HANS-FRIEDRICH WIRTH[b],
ASTRID GOLLWITZER[c], GERHARD GRAW[c],
RALF HERTENBERGER[c] and BERNHARD VALNION[c]

[a] *Nuclear Physics Institute, 250 68 Řež, Czech Republic*
[b] *Physik-Department, Technische Universität München, D-85748 Garching, Germany*
[c] *Sektion Physik, Universität München, D-85748 Garching, Germany*

Single γ-ray spectra and $\gamma\gamma$-coincidences, following thermal neutron capture in ^{124}Te, were measured with semiconductor detectors at the light-water reactor LWR - 15 at Řež. Intensities of γ transitions in ^{125}Te were normalized using the absolute intensity of 7.8% of the 6620 keV line in ^{36}Cl. The high resolution (d,p) measurements were performed with 17 MeV deuterons, using the Q3D spectrograph at two scattering angles of $15°$ and $30°$. Spectra were recorded in the range up to 3.3 MeV and calibrated using the proton peaks with l=1, and the corresponding level energies were determined in the thermal neutron capture reaction. The (^{3}He,α) experiment was carried out with a 32 MeV He beam at the angle of $10°$. The spectrum was recorded in one run by means of a large detector in a range up to approximately 4.7 MeV. The absolute intensities were determined by measuring the total beam current.

[1] Permanent address: Nuclear Research Center, LV 2169 Salaspils, Latvia; e-mail: brzs@lanet.lv

1. Introduction

The Te nuclei with only two protons beyond the closed shell $Z = 50$, span the wide neutron number region $N = 50 - 82$ ($A = 112 - 134$), allowing to investigate the evolution of the main nuclear structures if the number of valence neutron is gradually changed. One of them, the ^{125}Te nucleus, has been investigated in the past by various experimental methods [1]. In spite of the wide range of reactions employed in the previous studies, an insufficient accuracy and an incompleteness of data prevent a comprehensive analysis by modern theoretical models. In particular, very little is known on electromagnetic transitions between excited levels above 0.73 MeV. In this connection, it is interesting to note the surprisingly large cross-section of the 58 d ^{125m}Te long-lived isomer populated by the (γ, γ') reaction through the unknown doorway states at about 4 MeV excitation energy [2]. This curiously large value could be interesting for possible pumping a γ-ray laser [3]. In order to obtain a complete level scheme up to several MeV excitation energy, we performed the complex experimental study of this nucleus by the (n,γ), (d,p) and (^{3}He,α) reactions with greatly improved resolution and sensitivity. The present thermal neutron capture γ-ray and $\gamma\gamma$-coincidence studies on ^{125}Te were performed for the first time. Some preliminary results were published in Ref. 5. In order to preserve the superior quality and completeness of the accumulated data for further analysis and comprehensive theoretical interpretation, we decided to collect all these data in a separate issue. The experimental data presented here could be also useful for other applications including various nuclear data files. The construction and interpretation of the level scheme of ^{125}Te will be published later [6].

2. Thermal neutron capture studies

Single γ-ray spectra and $\gamma\gamma$-coincidences, following thermal neutron capture in ^{124}Te, were measured with semiconductor detectors at the light-water reactor LWR-15 at Řež. The target consisting of 1.2 g of metallic Te, enriched in ^{124}Te to 92.4%, was irradiated by thermal neutrons from a 6 m long neutron guide [4]. The beam was collimated to an area of 2.5 mm$\times$25 mm before hitting the target. The thermal neutron flux at the target position was 1×10^6 cm^{-2} s^{-1}.

Single γ-ray spectra were taken with a 22% HPGe detector with a resolution of 2.0 keV at the 1332 keV ^{60}Co line and 4.8 keV at 6534 keV over all periods of measurement. The detector pulses were processed with standard NIM electronics and stored in a PC. The centroid positions and peak areas were obtained by means of a computer program in which the peak shape was assumed to be gaussian, with a tail on the low-energy side. The low-energy part of the single spectrum is shown in Fig. 1. For calibration purposes, an auxiliary measurement has been performed with a mixed Te-Cl target. The energy calibration was made with well-known low-energy transitions in ^{125}Te [1], γ-rays from the ^{35}Cl(n,γ) reaction [7] and prominent background lines of ^{2}H and ^{60}Co. Intensities of γ-ray transitions in ^{125}Te were normalized using the absolute intensity of 7.8% of the 6620 keV line in ^{36}Cl [7]. A systematic error of 20% in the determination of absolute intensities in ^{125}Te is connected with the uncertainty of the capture cross-section of ^{124}Te [8]. In order to identify the γ-rays belonging to the ^{123}Te(n,γ) reaction, a separate run with a natural tellurium

target was performed. All γ-rays assigned to ^{125}Te with a possible placement in the level scheme are listed in Table 1.
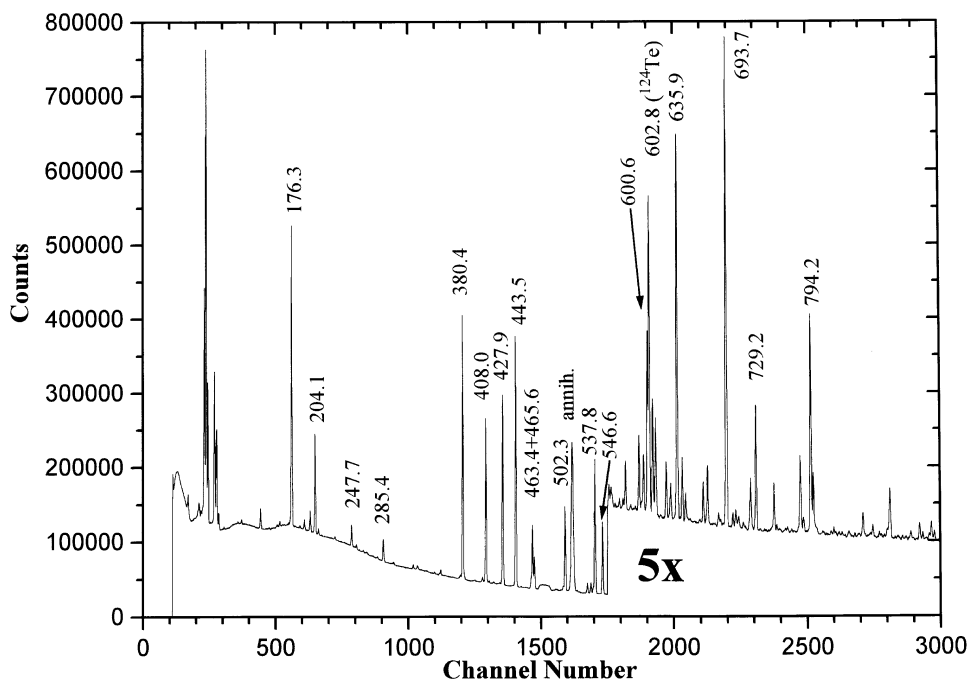
Fig. 1. The part of the single γ-ray spectrum from the reaction ^{124}Te(n,γ)^{125}Te. The peaks are marked by transition energies in keV.

TABLE 1. Gamma rays from thermal neutron capture in ^{124}Te.

E_γ^a (keV)	I $\frac{1}{(100n)}$	$\frac{\Delta I}{I}^b$ (%)	E_i^c (keV)	E_γ^a (keV)	I $\frac{1}{(100n)}$	$\frac{\Delta I}{I}^b$ (%)	E_i^c (keV)
176.30(5)	4.38	1.4	321.11	285.37(5)^d	0.50	3.0	1071.65
191.43(5)	0.15	2.1	729.22				729.22
204.14(4)	1.64	0.9	525.31	321.06(6)	0.10	3.9	642.21
208.09(5)	0.09	3.4	671.43	326.99(9)	0.04	11	–
227.91(5)	0.05	3.8	671.43	346.34(8)	0.05	10	1017.71
247.67(5)	0.40	1.3	1319.53	377.46(22)	0.08	33	1699.93
261.42(7)	0.04	7.9	786.72	380.44(5)	7.74	0.7	525.31
264.34(12)	0.02	16	1319.53	387.97(15)	0.02	20	–
265.88(7)	0.04	7.5	1319.53	394.63(9)	0.04	10	–

Table 1. (continued)

E_γ^a (keV)	I $\frac{1}{(100n)}$	$\frac{\Delta I}{I}^b$ (%)	E_i^c (keV)	E_γ^a (keV)	I $\frac{1}{(100n)}$	$\frac{\Delta I}{I}^b$ (%)	E_i^c (keV)
403.86(9)	0.13	12	1133.11	641.85(5)	0.68	1.2	786.72
408.04(5)	5.19	0.5	443.53	648.01(9)	0.04	9.1	1319.53
411.55(22)	0.05	33	1053.76	671.43(5)	0.66	0.9	671.43
427.85(5)	6.36	0.5	463.34	684.40(6)	0.15	4.1	1209.73
443.53(5)	8.82	0.6	443.53	686.67(8)^d	0.07	7.5	1357.53
449.82(9)	0.03	12	1092.4				2009.33
455.40(10)	0.02	13	–	693.72(5)	5.73	0.6	729.22
461.69(5)	0.35	1.7	1133.11	701.58(5)	0.15	3.4	1911.1
463.35(5)	2.30	0.3	463.34	704.94(5)	0.21	2.3	1242.94
465.55(5)	1.15	0.5	786.72	716.24(15)	0.03	19	1357.53
488.42(13)	0.02	24	–	721.24(10)	0.10	10	–
490.94(6)	0.06	5.1	1133.11	724.83(17)	0.04	18	–
497.35(17)	0.04	26	1133.11	729.22(5)	1.58	0.6	729.22
502.30(5)	3.33	0.4	537.79	739.24(23)	0.02	26	–
516.69(18)	0.04	26	1053.76	750.68(5)	0.62	1.1	1071.65
519.28(11)	0.03	19	(1652.50)	764.34(10)	0.05	11	1435.89
528.63(5)	0.42	1.4	1066.42	766.71(8)	0.07	6.1	2009.33
532.82(5)	0.45	3.1	1319.53	771.64(10)	0.04	12	1904.90
535.81(6)	0.27	4.8	1322.42	781.84(5)^d	1.07	1.9	1319.53
537.79(5)	5.83	0.4	537.79				1245.9
546.56(5)	3.14	0.6	1071.65	785.51(9)	0.20	9.2	2108.58
554.39(5)	0.20	2.5	1017.71	794.22(5)	3.02	0.5	1319.53
556.73(5)	0.13	4.0	1766.45	797.11(5)	0.82	1.3	1322.42
561.71(10)	0.04	14	–	799.27(11)^m	0.11	9.3	1242.94
566.86(6)	0.08	4.9	1699.93	801.17(13)^m	0.08	13	1265.16
571.37(6)	0.09	5.3	1242.94	809.94(9)	0.04	10	2129.60
574.17(5)	0.44	1.1	1017.71	818.38(8)	0.04	14	–
580.44(7)	0.04	10	(1652.53)	821.58(6)	0.11	4.4	1265.16
585.88(9)	0.04	11	(1652.53)	823.88(9)	0.05	9.8	–
590.39(5)^d	0.75	0.9	1053.76	827.82(9)	0.03	20	2150.1
			1319.53	839.19(9)	0.08	8.3	1911.1
593.58(7)	0.09	7.0	1265.16	840.75(21)	0.04	17	(1907.2)
595.78(5)	0.13	7.6	1133.11	850.28(23)	0.03	21	–
600.58(5)	1.77	1.2	636.07	851.87(18)	0.04	16	(2061.02)
606.70(5)	1.08	1.6	642.21	856.18(5)	0.36	1.7	1319.53
610.22(5)	0.94	1.8	1053.76	858.46(13)	0.04	15	1587.28
616.21(13)	0.03	15	–	865.39(10)	0.06	10	(1652.53)
22.88(5)^d	0.59	1.4	1066.42	875.85(8)	0.09	6.8	1319.53
			1832.32	878.28(10)	0.04	14	–
626.47(21)	0.03	26	1759.49	881.74(10)	0.05	9.8	2204.09
628.08(5)^m	0.37	1.9	1699.93	884.94(6)	0.13	4.5	1956.74
635.91(5)	4.15	0.8	671.43	887.11(6)	0.23	4.0	1529.71

Table 1. (continued)

E_γ^a (keV)	I $\frac{1}{(100n)}$	$\frac{\Delta I}{I}^b$ (%)	E_i^c (keV)	E_γ^a (keV)	I $\frac{1}{(100n)}$	$\frac{\Delta I}{I}^b$ (%)	E_i^c (keV)
888.56(5)	0.77	1.3	1209.73	1097.63(5)^m	1.13	1.1	1133.11
894.78(24)	0.02	27	1529.71	1115.23(9)	0.07	8.3	1652.53
903.18(10)	0.05	11	1956.74	1123.58(10)	0.06	10	1759.5
907.31(10)	0.05	9.4	1978.76	1130.53(11)	0.06	13	(1918.55)
911.04(18)	0.03	19	1435.89	1132.37(6)^d	0.25	3.2	2204.09
913.13(6)	0.14	4.3	1699.93				1670.16
915.95(15)	0.03	18	(1932.08)	1137.28(11)	0.06	9.5	(1580.8)
923.29(5)^d	0.29	2.4	1652.53	1139.61(8)	0.06	10	2270.83
			1994.8	1143.91(8)	0.09	6.4	1587.28
931.25(17)	0.04	23	–	1147.94(17)	0.04	15	–
937.47(5)	0.30	2.3	2009.33	1150.25(22)	0.03	21	–
940.94(6)	0.16	4.3	1670.16	1158.85(14)	0.07	12	–
950.24(24)	0.03	21	2649.65	1160.78(10)^d	0.10	8.4	1832.3
972.51(14)	0.08	13	(1435.89)				2226.18
975.41(6)	0.15	4.7	2047.5	1170.42(10)	0.11	8.0	1899.00
979.84(9)	0.10	8.1	(1766.45)	1175.46(6)^d	0.21	3.3	1904.90
981.72(9)	0.08	8.3	(1652.53)				2246.51
984.33(5)	0.29	2.4	1713.52	1182.65(9)	0.09	7.1	2315.6
992.39(9)	0.10	7.9	1435.89	1189.28(7)	0.13	5.5	1918.55
995.44(11)	0.05	13	2049.51	1194.81(14)	0.06	14	3106.07
998.49(7)	0.11	5.6	1670.16	1199.98(16)	0.12	16	–
1001.30(6)	0.16	3.8	1322.42	1207.29 (5)^d	1.12	0.9	1242.94
1004.86(9)	0.07	9.7	2076.95				3106.07
1010.53(12)	0.05	13	1652.53	1209.59(18)	0.06	14	1652.53
1014.53(10)	0.03	18	–	1211.91(15)	0.06	13	–
1018.36(5)	0.31	2.3	(1053.76)	1218.43(9)^m	0.06	8.5	2351.66
1027.52(23)	0.03	18	–	1225.19(20)	0.05	15	–
1029.33(17)	0.07	12	(1699.93)	1227.10(6)^d	0.26	3.5	1170.16
1030.92(5)	0.61	1.3	1759.5				1956.74
1036.73(5)	0.39	2.8	2108.58	1229.67(5)^d	0.87	1.0	1265.16
1042.12(6)	0.19	3.7	1713.52				2550.14
1045.52(15)	0.04	23	2310.75	1233.13(15)	0.05	20	1904.90
1049.35(15)	0.05	18	2292.9	1237.18(5)	0.35	2.3	(1775.0)
1054.19(7)	0.06	12	–	1241.11(10)	0.12	7.8	1766.45
1057.50(9)	0.09	7.9	(1521.16)	1242.92(5)	0.44	2.3	1242.94
1066.29(5)^d	0.66	2.0	1066.42	1247.6(3)	0.02	44	1918.53
			1529.66	1251.00(19)	0.04	20	–
1078.24(9)	0.08	7.9	2150.1	1255.4(3)	0.04	26	1699.93
1086.05(6)	0.29	4.2	1529.66	1257.07(16)	0.07	15	1899.00
1092.88(12)	0.06	13	2226.18	1261.00(12)^m	0.17	16	1932.1
1095.71(10)	0.06	19	2415.6	1262.18(15)	0.16	17	1990.0

Table 1. (continued)

E_γ^a (keV)	I $\frac{1}{(100n)}$	$\frac{\Delta I}{I}^b$ (%)	E_i^c (keV)	E_γ^a (keV)	I $\frac{1}{(100n)}$	$\frac{\Delta I}{I}^b$ (%)	E_i^c (keV)
1264.91(10)	0.08	8.0	1899.00	1477.84(22)	0.05	19	2550.14
1269.94(6)^d	0.23	3.0	1713.52	1493.30(6)	0.78	3.3	1956.74
			1904.90	1494.70(9)	0.37	6.8	1529.71
1274.60(18)	0.02	32	1813.0	1497.47(11)	0.11	9.4	2226.18
1284.22(9)^d	0.45	7.0	1319.53	1503.49(11)	0.08	12	2232.6
			1956.74	1509.29(19)	0.10	12	–
1286.6(3)	0.13	24	–	1511.4(3)	0.08	15	2181.93
1296.7(5)^d	0.13	24	1932.1	1513.33(6)	0.47	2.7	1956.74
			1759.5	1515.71(15)	0.08	12	2649.65
1307.26(5)^d	0.55	1.6	1771.16	1522.38(11)	0.08	9.1	2251.1
			1832.3	1528.89(10)	0.09	9.0	(1529.71)
1319.53(7)	0.36	5.1	1319.53	1535.02(11)^d	0.11	9.6	2607.02
1322.79(12)	0.19	9.4	1766.45				1978.76
1327.20(11)^m	0.27	8.6	1771.16	1538.70(19)	0.07	15	(1982.2)
1338.06(6)^d	0.21	4.4	2009.33	1541.4(3)	0.05	21	2270.83
			2410.1	1545.76(13)	0.09	11	2009.33
1342.35(12)	0.07	12	2585.76	1549.16(8)^m	0.23	4.9	2087.0
1347.94(18)	0.07	15	2076.95	1551.76(18)	0.08	15	1587.28
1349.71(7)^d	0.25	4.4	1813.0	1554.84(6)	0.36	3.4	2226.18
			2020.44	1565.91(11)	0.08	8.4	(2009.33)
1367.17(7)	0.16	5.1	1904.90	1575.28(24)	0.04	24	–
1378.66(9)	0.14	7.9	2049.51	1578.04(8)^m	0.28	5.0	2649.65
1382.69(11)	0.08	10	1918.53	1579.71(16)	0.10	14	2550.14
1385.82(9)	0.11	7.2	1911.1	1582.99(14)	0.13	12	2220.17
1388.19(21)	0.05	18	2061.02	1584.60(13)	0.16	9.3	(2313.64)
1395.41(17)	0.06	13	–	1587.27(5)	0.73	1.1	1587.28
1397.49(9)	0.13	6.1	2068.7	1591.84(8)	0.12	6.8	2129.60
1400.40(5)	0.51	1.6	(1435.89)	1598.93(7)	0.16	4.9	2270.83
1412.60(10)	0.60	1.8	2049.51	1605.99(6)	0.27	3.0	2049.51
1418.89(5)	0.60	1.8	1956.74	1611.56(24)	0.06	20	(2150.1)
1421.57(9)	0.17	5.7	1865.12	1617.51(5)	0.50	1.6	2061.02
1424.86(20)	0.06	27	2061.02	1621.59(9)^m	0.19	5.7	2351.66
1435.91(10)	0.05	28	(1899.00)	1631.91(18)	0.06	14	–
1437.61(13)	0.13	11	–	1634.4(3)	0.05	18	–
1440.94(5)	0.49	1.9	1978.76	1637.02(12)	0.09	8.7	–
1448.16(14)	0.08	14	1911.1	1641.32(24)	0.05	18	–
1452.91(11)	0.11	11	2181.93	1643.61(9)	0.20	5.6	2181.93
1455.42(7)	0.22	5.0	1899.00	1645.78(12)	0.13	8.8	–
1461.36(5)	0.35	2.0	1904.90	1650.30(8)	0.17	7.1	2379.47
1466.00(20)	0.06	16	–	1656.87(11)	0.10	9.9	2293.1
1470.64(20)	0.03	34	2009.33	1664.74(11)	0.12	7.8	2108.58
1475.03(6)	0.24	3.8	1918.53	1669.89(6)^m	0.31	2.9	2132.0

Table 1. (continued)

E_γ^a (keV)	I $\frac{1}{(100n)}$	$\frac{\Delta I}{I}^b$ (%)	E_i^c (keV)	E_γ^a (keV)	I $\frac{1}{(100n)}$	$\frac{\Delta I}{I}^b$ (%)	E_i^c (keV)
1678.17(14)	0.15	10	1713.52	1868.25(16)	0.15	12	–
1680.09(15)	0.19	7.5	2351.66	1870.03(15)	0.23	6.5	2313.6
1682.31(17)	0.10	12	2145.5	1872.00(17)	0.11	11	–
1686.18(6)^m	0.36	3.3	2129.60	1878.5(3)^m	0.11	27	2607.12
1688.45(18)	0.10	13	(2132.0)	1882.45(10)	0.13	9.0	1918.55
1699.87(11)	0.30	12	2770.65	1886.24(15)	0.07	18	–
1705.44(9)	0.10	9.8	–	1888.41(12)^d	0.15	7.9	2351.66
1708.90(10)^d	0.12	8.5	2379.47				3208.26
			2438.7	1897.09(9)	0.18	5.6	(2567.98)
1713.43(8)^m	0.37	4.3	1713.52	1899.4(3)	0.04	24	2438.7
1729.48(22)	0.05	25	–	1905.38(8)	0.38	4.2	1904.90
1732.87(7)^m	0.31	3.9	2270.83	1908.26(13)	0.16	6.8	2351.66
1735.39(13)	0.12	9.0	–	1910.50(15)	0.14	8.0	2372.6
1738.41(7)	0.24	4.1	2181.93	1913.09(11)	0.13	7.9	2438.84
1744.05(8)	0.18	6.3	2415.6	1919.55(12)^d	0.22	6.4	2649.65
1748.97(11)	0.07	11	–				1918.53
1753.08(15)	0.05	14	–	1921.59(9)^m	0.42	3.2	1956.74
1756.62(8)	0.13	5.3	–	1926.73(19)	0.06	22	–
1760.59(9)	0.12	5.8	(2204.09)	1928.79(6)	0.45	3.1	2466.59
1763.35(9)	0.09	7.5	2226.18	1933.20(9)	0.17	5.9	–
1766.18(9)	0.14	5.0	–	1935.80(22)	0.05	17	2379.47
1769.05(18)	0.03	21	(2438.7)	1939.16(9)	0.12	7.2	–
1775.32(13)	0.09	8.7	–	1942.81(10)	0.10	10	1978.76
1777.92(10)	0.10	30	2315.6	1950.18(14)	0.08	20	3021.3
1782.81(8)	0.13	7.5	2226.18	1954.01(15)	0.11	10	–
1788.02(7)	0.20	4.4	2232.6	1956.73(5)	2.76	0.5	1956.74
1795.12(9)	0.19	4.2	2466.58	1960.04(9)	0.16	8.3	–
1799.33(9)	0.12	6.7	2528.6	1967.16(17)	0.06	18	–
1807.22(9)	0.12	6.6	2250.8	1971.59(13)	0.11	8.6	(3291.1)
1827.28(13)	0.10	8.7	2270.83	1973.92(9)	0.19	5.2	2009.33
1829.68(9)^m	0.22	4.6	1865.12	1978.76(5)	0.50	2.0	1978.76
1832.17(20)	0.07	13	2560.73	1984.88(13)	0.11	9.9	–
1834.81(8)	0.17	5.5	2372.6	1990.79(20)	0.16	19	–
1838.42(12)	0.08	13	2567.98	1992.9(3)	0.15	22	–
1841.51(9)	0.10	11	2379.47	1994.6(3)	0.12	25	2438.84
1844.86(14)	0.07	20	–	2002.63(15)	0.11	13	2466.58
1849.41(23)^m	0.07	16	(2310.7)	2009.28(10)	1.53	1.4	2009.33
1851.54(9)	0.15	7.9	2315.64	2014.16(22)	0.10	22	(2550.14)
1855.4(3)	0.06	22	–	2018.25(17)	0.06	20	(2689.7)
1857.71(14)	0.11	11	2528.6	2022.92(13)	0.13	6.9	2466.58
1863.64(9)	0.38	6.9	1899.00	2025.52(19)	0.08	12	2061.02
1865.10(8)	0.43	6.3	1865.12	2032.14(10)	0.09	8.5	2495.4

Table 1. (continued)

E_γ^a (keV)	I $\frac{1}{(100n)}$	$\frac{\Delta I}{I}^b$ (%)	E_i^c (keV)	E_γ^a (keV)	I $\frac{1}{(100n)}$	$\frac{\Delta I}{I}^b$ (%)	E_i^c (keV)
2039.28(18)	0.10	12	(2674.30)	2233.01(21)	0.08	14	2770.71
2041.46(16)	0.16	7.6	2076.95	2235.56(12)	0.26	4.3	–
2044.34(21)	0.08	11	–	2245.30(19)	0.11	13	(2974.9)
2047.27(11)	0.41	2.7	2585.76	2247.15(16)	0.13	11	2246.51
2049.6(5)	0.04	26	(2495.4)	2252.0(2)	0.04	19	–
2052.27(13)	0.15	5.9	–	2268.2(4)	0.04	24	–
2058.8(3)	0.07	24	–	2270.49(17)	0.13	8.4	–
2060.67(21)	0.11	15	2504.2	2273.36(18)	0.12	8.1	3002.01
2066.08(25)	0.08	16	–	2275.6(3)	0.08	13	–
2068.01(17)	0.15	8.7	(2607.1)	2278.2(2)	0.07	13	2313.54
2070.68(11)	0.31	3.3	3142.25	2281.2(2)	0.10	13	–
2073.07(11)	0.27	3.7	2108.58	2283.16(18)	0.13	11	–
2077.04(10)^m	0.49	2.7	2076.95	2288.65(18)	0.16	7.7	–
2086.99(13)	0.13	6.8	2550.14	2291.3(2)	0.08	11	3021.26
2094.09(10)	0.56	1.8	2129.60	2296.1(3)	0.06	20	–
2098.58(18)	0.05	25	–	2302.62(13)	0.13	7.0	2974.9
2103.37(16)^m	0.12	9.9	3174.6	2305.51(13)	0.18	5.1	–
2106.25(19)	0.13	11	2550.14	2308.5(2)	0.10	11	2770.71
2108.41(13)	0.25	6.0	2108.58	2310.6(3)	0.08	14	–
2111.41(17)	0.10	11	–	2313.68(11)	0.34	2.9	2313.54
2124.66(15)^m	0.13	10	2568.0	2316.2(3)	0.11	18	2351.66
2128.12(13)	0.11	9.2	–	2317.9(3)	0.09	24	(2990.79)
2141.76(13)	0.23	8.3	2585.76	2328.1(2)	0.10	15	–
2146.69(23)	0.05	17	–	2330.3(2)	0.17	8.5	(3002.01)
2149.87(21)	0.13	13	(2819.7)	2332.85(12)	0.31	3.9	(2775.7)
2151.79(16)	0.21	7.5	–	2335.84(17)	0.12	8.4	2872.7
2161.23(24)	0.08	16	–	2342.24(17)	0.11	8.4	–
2163.17(26)	0.07	18	–	2345.2(3)	0.07	14	–
2168.81(16)	0.09	13	–	2348.2(2)	0.06	14	–
2173.76(20)	0.06	14	–	2351.75(13)^m	0.16	5.7	(2814.3)
2176.37(16)	0.08	9.5	–	2355.65(18)	0.08	12	(2819.7)
2182.41(20)	0.10	12	–	2370.18(12)^m	0.23	4.0	(2405.5)
2184.6(3)	0.08	16	2220.17	2378.1(3)	0.07	23	–
2186.69(11)	0.36	4.2	2649.65	2380.00(13)^d	0.25	6.0	2379.47
2190.71(11)^m	0.21	4.3	2226.22				2415.6
2193.85(24)	0.05	19	2729.64	2383.05(15)	0.13	6.7	–
2204.84(16)	0.10	13	2649.81	2393.6(2)	0.07	17	–
2208.43(21)	0.07	20	–	2396.92(13)	0.15	7.3	–
2211.25(13)	0.15	11	–	2400.5(2)	0.13	11	(3072.3)
2215.9(3)	0.10	22	(2754.1)	2402.90(16)	0.32	5.9	2438.84
2218.4(3)	0.10	22	–	2408.34(16)	0.11	12	–
2227.29(21)	0.11	16	–	2415.34(16)	0.08	11	–

Table 1. (continued)

E_γ^a (keV)	I $\frac{1}{(100n)}$	$\frac{\Delta I}{I}^b$ (%)	E_i^c (keV)	E_γ^a (keV)	I $\frac{1}{(100n)}$	$\frac{\Delta I}{I}^b$ (%)	E_i^c (keV)
2419.44(11)	0.23	3.9	–	2614.26(12)	0.17	17	2649.81
2422.54(15)	0.15	6.8	–	2616.2(3)	0.09	23	–
2425.1(2)	0.09	11	(2888.4)	2630.64(21)	0.06	17	–
2428.0(3)	0.08	18	–	2633.53(20)	0.10	8.7	–
2430.4(5)	0.13	35	2466.58	2644.59(20)	0.17	9.8	3106.07
2434.95(21)^m	0.08	13	3106.07	2659.3(4)	0.06	20	–
2454.17(15)	0.10	9.2	(3183.9)	2662.78(18)	0.11	14	3106.07
2458.4(2)	0.10	14	–	2670.59(12)	0.19	4.9	2705.9
2460.77(13)	0.21	6.8	2495.4	2674.24(10)^m	0.35	2.6	–
2467.03(13)^m	0.13	9.4	2466.58	2678.43(11)	0.27	3.4	–
2469.61(17)	0.11	11	–	2683.07(18)	0.08	11	–
2475.07(13)	0.28	6.9	–	2692.80(18)^m	0.19	8.5	(3231.7)
2477.0(3)	0.10	18	–	2696.62(23)	0.21	14	–
2480.14(12)	0.21	5.2	–	2699.01(20)	0.26	11	(3142.31)
2483.8(3)	0.06	27	3021.26	2705.6(3)	0.09	20	–
2485.8(5)	0.05	30	–	2716.33(12)	0.12	4.1	(2751.8)
2492.29(12)	0.17	4.7	(3563.5)	2719.82(11)	0.13	3.8	–
2495.38(11)	0.19	4.2	–	2730.55(15)^m	0.31	8.0	3174.2
2500.5(3)	0.04	21	–	2735.48(17)	0.15	9.2	2770.71
2509.1(3)	0.09	19	–	2751.1(4)^m	0.07	23	2785.83
2510.92(15)	0.18	11	2974.9	2767.26(15)	0.05	26	–
2514.62(13)	0.12	7.6	2550.14	2770.46(15)^m	0.10	6.8	2770.71
2518.56(16)	0.08	11	–	2781.83(21)	0.09	12	(2819.7)
2521.81(11)^m	0.23	3.5	–	2784.34(23)^m	0.09	14	2785.83
2525.04(14)	0.18	6.2	–	2792.92(15)	0.14	7.4	(3256.7)
2527.19(12)	0.24	4.6	2990.7	2799.30(14)	0.16	5.1	–
2532.81(11)	0.24	3.4	2568.0	2801.88(15)	0.12	7.6	(2801.9)
2539.40(23)	0.05	22	3002.01	2814.15(18)	0.08	11	–
2550.78(10)^m	0.39	2.6	2550.11	2827.67(11)	0.20	3.9	–
2554.71(14)	0.15	7.4	–	2846.27(12)	0.23	4.7	–
2557.38(13)	0.22	5.0	3021.26	2854.18(15)	0.16	7.3	(2854.7)
2560.66(17)	0.10	13	2560.9	2862.65(10)	0.25	3.2	–
2566.1(2)	0.10	12	–	2869.4(3)	0.06	21	–
2568.72(13)^m	0.20	6.0	2568.0	2873.58(20)	0.05	21	–
2571.92(16)	0.11	8.9	2607.1	2876.93(15)	0.17	6.6	–
2577.85(14)	0.13	8.3	3021.26	2885.0(3)	0.05	25	(2919.7)
2580.72(11)	0.20	6.1	–	2893.97(11)	0.16	5.1	–
2589.81(23)	0.11	13	–	2898.00(10)	0.16	8.0	(2898.4)
2593.55(15)	0.16	7.5	–	2902.38(15)	0.12	5.6	(2938.3)
2597.50(15)	0.16	6.9	–	2906.1(3)	0.05	13	–
2607.01(12)	0.19	5.2	2607.1	2914.07(21)	0.08	10	–
2609.64(10)	0.45	3.4	–	2916.86(10)^m	0.24	4.7	6568.97

Table 1. (continued)

E_γ^a (keV)	I $\frac{1}{(100n)}$	$\frac{\Delta I}{I}^b$ (%)	E_i^c (keV)	E_γ^a (keV)	I $\frac{1}{(100n)}$	$\frac{\Delta I}{I}^b$ (%)	E_i^c (keV)
2922.25(23)	0.05	12	–	3238.39(15)	0.10	18	–
2925.67(15)	0.09	7.9	–	3242.0(4)	0.07	18	–
2933.18(20)	0.20	11	–	3251.81(12)	0.18	4.5	–
2935.34(15)	0.25	9.2	–	3263.91(15)	0.09	8.6	–
2939.98(11)	0.05	27	2974.9	3278.37(11)	0.29	3.5	(6568.97)
2943.5(3)	0.06	23	–	3291.83(14)	0.15	5.2	(3291.1)
2956.05(10)	0.50	2.4	2990.7	3301.58(15)	0.12	8.3	–
2964.55(15)	0.18	6.0	–	3311.88(12)	0.13	5.5	(6568.97)
2969.92(20)	0.08	13	–	3332.68(23)	0.13	9.0	–
2977.3(4)	0.07	20	–	3336.25(17)	0.17	7.1	(6568.97)
2980.38(15)	0.19	7.4	–	3345.3(3)	0.05	15	–
2986.37(15)	0.18	6.2	3021.26	3350.26(12)	0.16	5.2	–
2990.02(15)	0.12	10	2990.7	3360.82(10)	0.54	2.0	6568.97
3005.68(12)	0.23	5.6	6568.97	3373.86(14)	0.11	5.5	(6568.97)
3014.40(11)	0.28	4.0	6568.97	3378.66(18)	0.07	9.1	–
3022.27(20)	0.09	13	3021.26	3385.02(10)	0.24	2.9	(6568.97)
3036.76(11)^m	0.22	11	(3072.3)	3394.48(11)	0.48	3.4	(6568.97)
3043.69(21)	0.12	15	–	3405.6(3)	0.08	16	–
3057.33(12)	0.10	12	–	3426.73(10)	0.43	2.1	6568.97
3068.27(11)	0.24	4.5	–	3432.09(20)	0.07	11	(6568.97)
3078.01(21)	0.10	10	–	3459.06(18)	0.15	9.5	–
3080.73(14)	0.19	5.2	–	3463.04(10)	0.61	2.3	6568.97
3089.1(3)	0.10	14	3532.7	3496.54(10)	0.27	3.0	6568.97
3092.10(20)	0.14	12	3554.2	3501.63(12)	0.17	4.1	–
3096.24(20)	0.12	13	–	3547.72(10)	0.58	2.9	6568.97
3101.5(3)	0.06	21	–	3554.28(15)^m	0.25	7.3	(3554.1)
3106.41(10)^m	0.25	3.9	3106.07	3567.25(10)	0.25	7.9	6568.97
3120.63(20)	0.11	10	–	3574.6(5)	0.09	24	–
3125.85(11)	0.27	4.0	–	3577.86(20)	0.24	9.4	6568.97
3130.61(20)	0.06	25	–	3594.2(7)	0.07	29	6568.97
3138.67(10)	0.47	2.5	–	3617.41(14)	0.16	5.2	–
3142.48(18)	0.15	8.2	3142.31	3630.20(20)	0.08	10	(6568.97)
3164.78(14)	0.15	5.4	–	3648.32(13)	0.18	5.5	6568.97
3168.28(12)	0.06	19	–	3652.24(20)	0.10	8.7	–
3174.07(15)	0.09	14	(3208.26)	3660.9(3)	0.04	17	–
3180.3(4)	0.04	25	–	3665.1(3)	0.04	18	–
3184.20(15)	0.15	6.8	3183.9	3670.71(15)	0.08	7.5	(6568.97)
3192.7(3)	0.05	14	–	3696.30(15)	0.05	9.4	6568.97
3207.84(14)	0.14	5.6	3208.26	3706.35(12)	0.06	18	–
3210.89(12)	0.17	4.8	3652.5	3713.4(3)	0.05	16	–
3219.01(11)	0.34	4.2	–	3745.3(4)	0.07	13	–
3223.75(18)	0.15	9.7	–	3749.48(12)	0.24	2.9	(6568.97)

Table 1. (continued)

E_γ^a (keV)	I $\frac{1}{(100n)}$	$\frac{\Delta I}{I}^b$ (%)	E_i^c (keV)	E_γ^a (keV)	I $\frac{1}{(100n)}$	$\frac{\Delta I}{I}^b$ (%)	E_i^c (keV)
3755.13(21)	0.07	8.8	(6568.97)	4387.25(14)	0.06	12	6568.97
3766.89(20)	0.05	11	–	4393.1(3)	0.04	14	6568.97
3779.4(5)	0.07	21	–	4422.52(24)	0.03	36	6568.97
3782.98(16)	0.28	5.7	6568.97	4439.39(11)	0.50	2.2	6568.97
3793.37(24)	0.10	14	(6568.97)	4460.35(11)	0.67	1.9	6568.97
3798.26(12)	0.44	3.2	6568.97	4492.19(10)	0.25	2.4	6568.97
3813.9(3)	0.08	11	–	4508.05(11)	0.22	2.7	6568.97
3817.2(3)	0.07	11	6568.97	4519.8(3)	0.04	14	6568.97
3839.46(21)	0.16	9.7	6568.97	4559.56(10)	1.75	1.7	6568.97
3863.33(13)	0.12	5.1	(6568.97)	4590.18(11)	0.62	1.8	6568.97
3879.01(18)	0.13	6.4	(6568.97)	4612.14(11)	4.23	2.1	6568.97
3890.57(12)	0.12	3.4	–	4663.84(13)	0.15	4.5	6568.97
3894.67(11)	0.21	2.8	–	4669.88(18)	0.08	7.7	6568.97
3919.33(10)	0.87	1.4	6568.97	4703.74(14)	0.14	5.1	6568.97
3961.57(14)	0.32	7.3	6568.97	4809.2(6)	0.07	19	6568.97
3982.95(4)	0.49	1.8	6568.97	4855.44(11)	0.22	2.3	6568.97
4001.05(11)	0.41	2.7	6568.97	4869.8(7)	0.02	30	6568.97
4008.15(18)	0.10	10	(6568.97)	4898.52(15)	0.07	13	6568.97
4018.90(12)	0.46	3.2	6568.97	4916.32(17)	0.09	9.6	6568.97
4074.6(3)	0.07	14	(6568.97)	4981.59(12)	0.23	3.1	6568.97
4102.65(10)	0.26	5.4	6568.97	5039.42(13)	0.14	4.2	6568.97
4130.2(3)	0.05	14	6568.97	5133.5(5)	0.02	23	6568.97
4153.02(13)	0.07	8.2	6568.97	5249.28(10)	3.66	1.5	6568.97
4158.92(16)	0.06	9.8	6568.97	5303.77(16)	0.14	5.8	6568.97
4164.03(26)	0.05	13	–	5326.0(6)^e	0.07	14	6568.97
4189.37(13)	0.34	4.1	6568.97	5502.4(2)^e	0.08	25	6568.97
4217.7(3)	0.25	13	6568.97	5514.2(2)^e	0.10	20	6568.97
4253.70(13)	0.23	3.5	6568.97	5839.65(11)	1.78	2.0	6568.97
4297.84(18)	0.09	7.7	6568.97	6030.8(4)	0.31	16	6568.97
4318.0(3)	0.05	14	6568.97	6125.42(10)	1.15	1.0	6568.97
4322.32(26)	0.07	10	6568.97	6533.56(11)	3.23	2.1	6568.97
4342.96(11)	0.61	2.0	6568.97	6569.07(11)	1.61	2.0	6568.97
4364.7(3)	0.05	17	6568.97				

^{a}Numbers in parentheses denote the uncertainties of the last digits. They include statistical and systematical errors.

^{b}Statistical error is given. 20% systematical error in consequence of uncertainty of capture cross-section must be take into account.

^{c}Energy of initial state. Brackets express uncertain placement.

^{d}Unresolved doublets.

^{e}Energies and intensities from single or double escape peaks.

^{m}Multiplacement. Only principal component is given.

3. Light-ion induced reactions

The experiments were performed at the Tandem Accelerator of the University and Technical University of Munich. The reaction products were analyzed in the Q3D spectrograph [9] equipped with a position-sensitive cathode-strip detector with single-strip read-out [10,11] and a long-focal-plane detector with trace reconstruction [12].

The (d,p) measurements were performed with 17 MeV deuterons at two scattering angles of 15° and 30°. This allows partly to avoid the problem of interference of Te peaks with background peaks. The 90.7% enriched target of ^{124}Te had dimensions of 1×4 mm^2 and a thickness of 40 μg/cm^2 on a 4.7 μg/cm^2 thick carbon backing. Several spectra were recorded in the range up to 3.3 MeV by taking 7 overlapping runs, each about 700 keV wide. The example of the proton spectrum is given in Fig. 2. The intrinsic position precision is better than 0.1 mm which makes
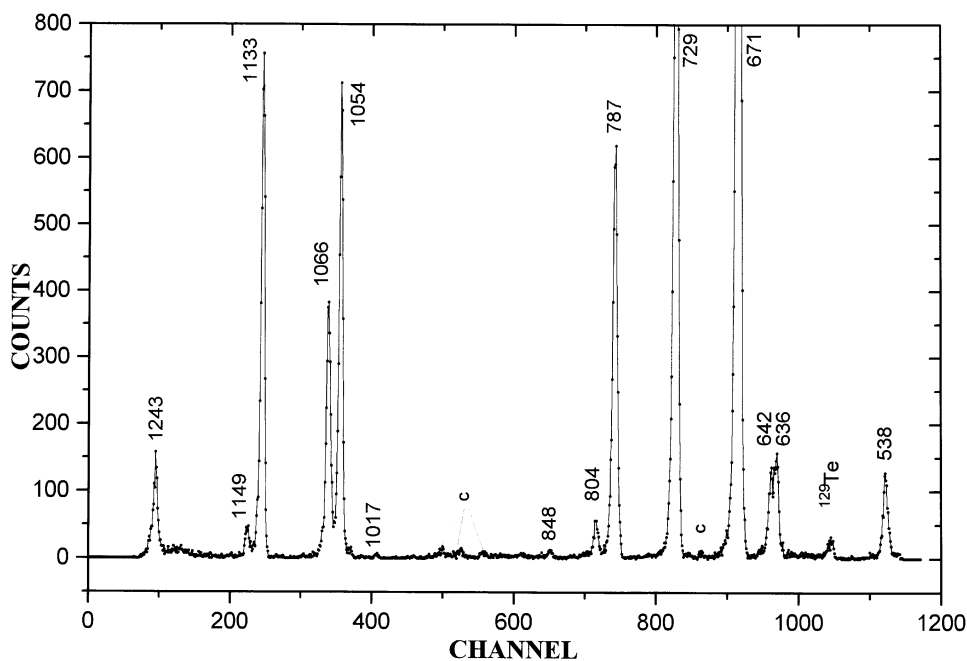
Fig. 2. The proton spectrum at the angle of 15° from the reaction ^{124}Te(d,p)^{125}Te, using 17 MeV deuteron beam. The peaks are marked by corresponding level energies in ^{125}Te.

it possible to determine the energy of strongest peaks with a precision up to 0.1 keV with an energy resolution of about 4 keV (FWHM). This resolution is about 3 times better than in the previous (d,p) measurement [13]. Each run was calibrated using corresponding level energies determined in the thermal neutron capture reaction.

TABLE 2. Levels of ^{125}Te observed in the (d,p) reaction at a beam energy of 17 MeV and at angles of 15° and 30°.

Energy[a] (keV)	Relative Intensity $\Theta = 15°$	$\Theta = 30°$	Energy[a] (keV)	Relative Intensity $\Theta = 15°$	$\Theta = 30°$
0.1(2)		6520(150)	1715.7(6)	13(2)	
35.40(20)		4770(130)	1759.78(27)	44(4)	
145.13(11)	845(17)	2121(87)	1770.59(27)	42(4)	
443.3(4)	416(12)	140(23)	1813.0(5)	461(19)	107(15)
462.8(4)	52(5)	50(17)	1820.2(4)	755(24)	510(27)
525.28(12)	164(8)	146(26)	1824(1)	c	39(8)
537.74(10)	172(5)	277(33)	1863.4(5)	c	82(12)
636.17(9)	184(7)	230(33)	1888(1)	c	14(6)
641.56(11)	134(6)	310(37)	1905.2(7)	c	44(10)
671.25(8)	2664(31)	1773(80)	1918.6(8)	c	20(7)[h]
685.1(6)[b]	15(3)		1929.4(6)	c	543(98)[h]
705.3(6)[d]	5.2(17)		1956.72(15)	819(27)	660(150)[h]
729.05(6)	1650(17)	823(53)	1966.7(5)	27(6)	
786.78(8)	793(11)	877(56)	1982.3(6)	785(22)	798(54)[h]
804.61(14)	68(4)	37(17)	1994.6(6)	62(8)	386(68)[h]
847.90(29)[d]	12(2)		2009.77(22)	252(12)	369(35)
1017.6(5)	5.4(11)		2049.14(28)	1865(23)	2358(58)
1053.72(9)	710(10)	520(40)	2061.4(5)	21(5)	
1066.16(18)	445(8)	348(35)	2079.5(4)	47(5)	60(13)
1133.11(10)	730(21)	722(50)	2112.5(4)	4071(33)	6900(100)
1148.73(21)	42(3)	115(20)	2126.8(4)	1184(18)	2623(63)
1203.9(11)[e]		31(12)	2153.4(5)	71(5)	c
1243.3(4)	120(19)[h]	57(15)	2187.7(4)	204(8)	1020(140)[h]
1265.15(20)	304(36)[h]	287(30)	2206.9(5)	25(4)	c
1277.7(5)	43(11)		2223.9(5)[e]	15(4)	c
1315.0(4)	19(4)	53(17)	2250.1(4)	539(13)	800(110)[h]
1319.71(13)	167(6)	194(27)	2274.2(4)[e]	96(6)	c
1357.62(27)	27(3)	83(22)[h]	2282.6(4)	59(6)	c
1427.90(23)[b]	12 (3)		2305.2(6)[g]	24(5)	c
1435.81(11)	218(7)	186(28)[h]	2315.6(4)	1787(58)	2690(150)[h]
1520.3(5)	5.2(22)		2332.7(4)	346(11)	960(140)[h]
1529.85(9)	171(6)	103(12)	2338.6(7)	37(7)	c
1536.3(7)[b]	5(2)		2351.7(4)	236(9)	c
1551.3(7)[b]	7(2)		2375.41(26)	82(5)	143(18)
1558.8(7)[b]	6(2)		2382.0(4)	49(5)	
1581.0(4)	15(2)		2391.1(4)	84(10)	125(7)
1587.20(10)	184(8)	443(23)	2398.1(9)[e]	26(4)	34(5)
1652.4(5)	9.6(18)	25(9)	2412.3(4)	35(4)	38(5)
1670.5(6)	8.5(18)		2419.1(3)	81(8)	121(7)
1700.09(15)	450(10)	475(26)	2426.2(9)	28(4)	41(5)

Table 2. (continued)

2439.3(5)	27(3)	28(4)	2852.3(5)	99(20)	c
2450.62(28)	42(4)	53(5)	2860.8(5)	44(5)	c
2457.9(7)	17(3)	36(5)	2868.4(7)	34(5)	c
2465.84(29)	117(6)	145(7)	2874.3(8)	23(4)	c
2605.5(7)	c	53(5)	2881.5(8)	21(4)	c
2479.06(29)	22(4)	32(4)	2888.5(4)	134(9)	c
2488.36(29)	104(6)	129(7)	2900.0(6)	141(9)	c
2495.0(7)	29(5)	39(5)	2910.0(5)	118(9)	c
2521.0(4)	161(8)	208(8)	2927.3(7)	34(6)	c
2525.7(5)^f	24(7)		2932.7(7)	112(9)	c
2542.0(4)	45(9)	106(7)	2938.5(7)	49(6)	c
2547.2(7)	c	35(5)	2950.0(7)	59(7)	c
2556.8(7)	c	43(5)	2965.4(7)	273(11)	c
2590.4(7)	c	151(8)	2988.6(6)	60(7)	128(20)
2596.0(7)	c	69(6)	3008.2(5)	39(7)	61(7)
2622.6(6)	c	389(12)	3015.1(7)	34(7)	73(7)
2630.5(6)	c	175(8)	3022.6(6)	50(7)	38(6)
2642.4(6)	c	393(12)	3032.0(5)	217(13)	165(30)
2651.3(7)	c	35(5)	3044.9(8)	89(10)	≈ 80
2669.7(6)	c	300(10)	3060.2(5)	206(11)	175(33)
2680.2(7)	c	40(5)	3071.0(5)	94(8)	121(30)
2684.8(7)	c	42(5)	3082.3(8)	43(7)	
2690.1(7)	c	32(5)	3090.9(5)	203(11)	202(33)
2704.6(4)	98(8)	134(6)	3098.3(7)	147(10)	
2711.6(4)	37(7)	53(5)	3130.1(4)	c	362(39)
2717.3(4)	23(5)	36(4)	3143.3(4)	c	317(38)
2723.1(5)		41(4)	3151.0(8)	c	138(30)
2730.2(4)	39(7)	65(5)	3169.5(5)	149(28)	175(32)
2743.1(4)	93(20)	114(5)	3189.4(12)	118(18)	163(30)
2748.63(29)	484(56)	700(13)	3201.0(6)	106(19)	127(25)
2761.5(4)	102(25)	144(7)	3210.6(6)	81(18)	135(25)
2768.07(28)	393(49)	476(12)	3218.6(11)	59(16)	
2773.3(4)	63(17)	71(8)	3235.5(10)	68(14)	
2784.2(4)	55(9)	78(13)	3259.8(7)	220(13)	238(55)^h
2804.6(4)	128(12)	187(14)	3272.7(12)	82(8)	
2816.7(7)	97(10)	c	3297.5(10)	76(7)	240(66)^h
2832.1(5)	112(21)	c	3329.5(9)		124(28)
2840.8(5)	200(25)	c			

^{a}Weighted average of two angles measurements.

^{b}Unknown contaminant.

^{c}Completely obscured by a broad contaminant peak.

^{d}Partly belongs to ^{123}Te.

^{e}Possibly belongs to ^{127}Te.

^{f}Partly belongs to ^{129}Te.

^{g}Possibly belongs to ^{131}Te.

^{h}Superimposed onto a broad contaminant peak.

Individual runs were sewn using data from a monitor counter (Si telescope detector) which recorded the elastically scattered particles at a fixed angle of 40°. Some minor contamination from other Te isotopes has been subtracted using well-known Q-values and assuming that the relative intensities of contaminant peaks follow those reported previously [14–16,13]. Weighted mean energies and corresponding relative intensities of the (d,p) peaks at two angles are listed in Table 2.

The (^{3}He,α) experiment was performed with a 32 MeV He beam at only one angle of 10°. The effective thickness of the target of 97.8% enriched ^{126}Te was 60 μg/cm^2. This spectrum was recorded by a large detector in a wide range up to approximately 4.7 MeV [12]. The energies were determined by a polynomial least-squares fit procedure using the accurate energies of the low-lying states obtained in the (d,p) study. Above 3.3 MeV, this energy calibration becomes much less reliable due to the lack of accurate energy points. Therefore, for these energies the intrinsic high position-sensitive precision of the large detector could not be fully realized. An energy resolution of about 18 keV (FWHM) for the single α-peaks at lowest excitations was obtained. Few contaminant peaks from other Te isotopes have been identified by comparison with the calculated energies using the Q-values from the Wapstra tables and the known spectroscopic information on tellurium isotopes. The absolute cross-sections were determined by measuring the total beam current into a Faraday cup. Energies and cross-sections of the observed discrete α-peaks are listed in Table 3.

TABLE 3. Levels of ^{125}Te observed in the (^{3}He,α) reaction at a beam energy of 32 MeV and at an angle $\Theta = 10°$.

Energy (keV)	Intensity (microbarn/sr)	Energy (keV)	Intensity (microbarn/sr)
36.5(19)	48(4)	1357.8(14)	28.8(24)
145.0(11)	1035(43)	1378.3(30)[d]	3.4(12)
317(4)[a]	11.6(15)	1434.5(14)	31.2(26)
446(4)[b]	6.9(21)	1527.2(16)	14.4(19)
464(3)	4.8(17)	1583.4(19)[e]	9.6(15)
521(4)	6.7(14)	1643.3(26)	5.3(12)
639.4(21)	339(79)	1661.5(26)	3.9(17)
667(3)	58(4)	1698.9(26)	4.3(17)
786(4)	15.1(26)	1725.8(14)[g]	77(4)
803(4)	17.6(26)	1757.7(19)[g]	13.2(17)
1026.0(42)[c]	2.7(12)	1813.8(28)	14(5)
1054.3(12)	56(4)	1826.4(28)	11(4)
1086.3(25)	6.3(14)	1885.5(28)	6.7(24)
1117(3)[d]	4.7(13)	1909.0(19)	23(4)
1135.7(14)	38(4)	1922.0(28)	12(3)
1152.9(17)	26(4)	1968.2(21)[e]	19(5)
1237.0(20)[e]	10.3(17)	2007.1(14)[g]	20.2(24)
1264.8(13)	54(4)	2045(3)	5.7(21)
1315.6(13)[f]	60(4)	2082.2(14)	19.4(24)

Table 3. (continued)

Energy (keV)	Intensity (microbarn/sr)	Energy (keV)	Intensity (microbarn/sr)
2104.8(29)	6.4(21)	2772(4)^e	14.3(36)
2159.9(21)	11.3(21)	2847(5)	8.9(24)
2189.5(21)^e	12.5(21)	2911(5)	6.2(21)
2226(3)	6.7(21)	2966(4)	13.7(24)
2259.4(24)^g	8.8(21)	3005(5)	7.2(21)
2316.5(22)	10.0(21)	3049(4)^e	20.1(27)
2364(3)	7.8(21)	3105(5)^h	1.5(11)
2388.8(26)	8.2(21)	3164(4)^h	3.4(17)
2427(4)	7.4(21)	3215(4)^h	3.8(18)
2449(3)	9.1(21)	3339(5)^h	8.1(21)
2492(4)	4.3(21)	3375(5)^h	6.3(19)
2530(4)	6.5(21)	3488(5)^h	4.1(18)
2557(4)	6.9(21)	3564(5)^h	4.4(19)
2582.1(28)^g	14.2(24)	4208(5)^h	2.7(12)
2641.5(24)	17.3(26)	4302(4)^h	2.4(12)
2678(5)	6.9(21)	4481(4)^h	3.6(12)
2733(4)	5.7(21)	4513(4)^h	5.3(14)

^{a}Possibly perturbed by transition in ^{123}Te.

^{b}Perturbed by transition in ^{127}Te.

^{c}Possibly perturbed by an unknown contaminant.

^{d}Unknown contaminant.

^{e}Complex structure.

^{f}There are unknown contaminant peaks on both tails.

^{g}Doublet structure.

^{h}Uncertainties of the energy values could raise up faster than quoted due to the lack of calibration points at higher energies.

4. Angular-correlation effect in thermal neutron capture

In our coincidence measurements, we observed a strong $\gamma\gamma$-correlation effect which is manifesting itself by the deviation of some branching ratios in the $\gamma\gamma$-coincidence spectra relative to the single γ–spectrum. A remarkably large difference (see Table 4) by a factor of 2 is observed for the pair of the 408 and 443 keV transitions going from the $3/2^+$ level at 443 keV, gated by the primary transition of 6125 keV from the $1/2^+$ capture state to this level. No similar effect is observed for the neighbouring $1/2^+$ level at 537 keV since the angular distribution of the secondary γ-rays in this case must be isotropic.

For a more detailed analysis of the $\gamma\gamma$-correlations in our close geometry with the angles between detectors of $180°$ [4], we calculated the product of attenuation coefficients for the pair of the γ–ray detectors and obtained the reasonable value of $Q_2(1)Q_2(2) \approx 0.6$. However, using this value, and assuming a pure primary dipole transition and mixed E2/M1 secondary ones with signs and magnitudes of mixing ratios recommended in Ref.

17, we were not able to reproduce the experimental value of 1.12(9). A good agreement between the expected and experimental branchings in this case could be achieved only if we suppose:

(i) the primary transition is pure dipole and secondary ones are of mixed E2/M1 type but with signs opposite to those obtained in the Coulomb excitation work cited in Ref. 17.

(ii) the primary transition is mixed E2/M1 but the mixing ratios as well as the signs for the secondary transitions are in accord to those recommended in Ref. 17.

The latter seems unexpected since the observed value of $(E2/M1 \equiv \delta \approx -1)$ for the primary transition in this case would require an unusually large E2 strength which contradicts the known recommended upper limit [18].

TABLE 4. *Comparison of branching ratios for some secondary transitions observed in the present and others studies.*

Branching ratio	Ref.[1]	Present work		
		In single sp.	In coincidences with several gates	
$I_\gamma(408)/I_\gamma(443)$	0.61(1)	0.588(6)	1.12(9)^a	
$I_\gamma(502)/I_\gamma(537)$	–	0.572(4)	0.51(8) 0.52(6) 0.53(6) 0.57(7)	

^{a}Gated by primary transition

5. Conclusions

The present complex experimental study of ^{125}Te with (n,γ), (d,p) and (^{3}He,α) reactions has yielded extensive spectroscopic material. In total, 645 γ-lines were ascribed to the ^{125}Te nucleus in the (n,γ) experiment. In the (^{3}He,α) and high resolution (d,p) experiments, 2 to 3 times more levels have been observed in comparison with previous studies.

A difference in the 408/443 keV branching ratio determined from single and coincidence γ-ray spectra was observed. This difference can be satisfactory explained only if one assumes a strong E2 admixture in the 6125 keV primary transition. To clear up this question, there is evidently the need for a γ-γ angular correlation measurement.

Acknowledgements

References

1) J. Katakura, M. Oshima, K. Kitao and J. Iimura, Nucl. Data Sheets **70** (1993) 217;

2) J. J. Caroll, T. W. Sinor, D. G. Richmond, K. N. Taylor, C. B. Collins, M. Huber, N. Huxel, P. v. Neumann-Cosel, A. Richter, C. Spieler and W. Ziegler, Phys. Rev. **C43** (1991) 897;

3) C. B. Collins, F. W. Lee, D. M. Shemwell, B. D. DePaola, S. Olariu and I. I. Popescu, J. Appl. Phys. **53** (1982) 4645;

4) J. Honzátko, K. Konečný, I. Tomandl, J. Vacík, F. Bečvář and P. Cejnar, Nucl. Instr. and Meth. **A376** (1996) 434;

5) V. Bondarenko, J. Honzátko and I. Tomandl, Z. Phys. **A354** (1996) 235;

6) J. Honzátko et al., to be published;

7) B. Krusche, K. P. Lieb, H. Daniel, T. von Egidy, G. Barreau, H. G. Börner, R. Brissot, C. Hofmeyr and R. Rascher, Nucl. Phys. **A386** (1982) 245;

8) S. F. Mughabghab, M. Divadeenam and N. E. Holden, *Neutron Cross Sections*, Vol.1, part A (Academic Press New York 1981);

9) M. Löffler, H. J. Scheerer and H. Vonach, Nucl. Instr. and Meth. **111** (1973) 1;

10) H. Lindner, H. Angerer and G. Hlawatsch, Nucl. Instr. and Meth. **A273** (1988) 444;

11) J. Ott, H. Angerer, T. von Egidy, R. Georgii and W. Schauer, Nucl. Instr. and Meth. **A367** (1995) 280;

12) E. Zanotti, M. Bisenberger, R. Hertenberger, H. Kader and G. Graw, Nucl. Instr. and Meth. **A310** (1991) 706;

13) A. Graue, J. R. Lien, S. Røyrvik, O. J. Aarøy and W. H. Moore, Nucl. Phys. **A136** (1969) 513;

14) A. Graue, E. Jastad, J. R. Lien, P. Torvund and W. H. Moore, Nucl. Phys. **A103** (1967) 209;

15) W. H. Moore, G. K. Schlegel, S. O' Dell, A. Graue and J. R. Lien, Nucl. Phys. **A104** (1967) 327;

16) A. Graue, E. Hvidsten, J. R. Lien, G. Sandvik and W. H. Moore, Nucl. Phys. **A120** (1968) 493;

17) K. S. Krane, Atomic Data and Nuclear Data Tables **19** (1977) 299;

18) J. Kopecky, in *Proc. 4th Int. Symp. on Capture Gamma-Ray Spec. and Related Topics*, ed. T. von Egidy, Grenoble, France (1981) p. 426.

SPECTROSCOPIJA ^{125}Te (n,γ), (d,p) I (^{3}He,α) REAKCIJAMA

Mjerili su se izravni γ- i sudesni γ-γ-spektri nakon uhvata termičkih neutrona u ^{124}Te. Mjerenja (d,p) reakcija visokog razlučivanja na toj jezgri izvela su se s deuteronima 17 MeV na kutovima od 15° i 30°, pomoću Q3D spektrografa. Također se mjerio spektar u reakciji (^{3}He,α) na 10°. Na osnovi tih mjerenja utvrđena su mnoga nova stanja ^{125}Te na energijama uzbude do oko 4.5 MeV. Razlika grananja 403/443 keV iz izravnih i sudesnih γ-spektara ukazuje na jaku primjesu E2 u primarnom prijelazu od 6125 keV.